Dependence of quasi-helical symmetry and quasi-axisymmetry on magnetic axis torsion and magnetic surfaces ellipticity

S. Guinchard*
Section de Physique, Ecole Polytechnique Fédérale de Lausanne, Lausanne, Suisse
(Supervised by A. Baillod and J. Loizu)†
(Dated: June 20, 2022)

In this document, some properties of magnetic coordinates are studied in several coordinate systems. Transformation from general poloidal and toroidal angles to Boozer coordinates, via general straight field lines coordinates is reviewed. Boozer coordinates have been implemented numerically in the booz xform code [Lan18], to be evaluated over SPEC equilibria, in order to quantify the influence of magnetic axis torsion and flux surfaces ellipticity on quasi-symmetry properties, in particular quasi-helical symmetry and quasi-axisymmetry.

Keywords: Stellarator, quasi symmetry, torsion, ellipticity, quasi-axisymmetric stellarator, quasi-helical symmetric stellarator, shear, shearless

I. INTRODUCTION

Stellarators are magnetic confinement devices that hold promises to confine plasmas with sufficient efficiency to achieve net production of electricity by nuclear fusion. Although they do not present many of the current-driven instabilities present in tokamaks, their optimisation constitutes however a tremendous task [Gui22]. Indeed, confining hot plasmas using specific and appropriate magnetic fields is one of the main challenges of plasma physics research. Hence, magnetic confinement configurations design requires careful consideration for the particles to be confined effectively [RSB22].

A promising confinement concept is the *quasi-symmetric stellarator*. Quasi-symmetric stellarators possess the remarkable property that the magnitude of the magnetic field $\|B\|$ is symmetric, even whenever $\mathbf{B}$ is not [RSB22, LSP19]. Quasi-symmetric stellarators guarantees good neoclassical transport [CS97]. Although perfect quasi-symmetry seems not possible to be achieved, it remains possible to exhibit behavior close to quasi-symmetry in a volume [RSB21]. However, quasi-symmetries are not obvious, since they depend on the choice of the coordinate system in which the magnetic field is represented. This property is hence characterised as a *hidden symmetry*. In addition to quasi-symmetry property, the configuration should preferably be in a state of magnetohydrodynamic (MHD) equilibrium [RSB22]. For fusion plasmas, this is expressed by the balance between the plasma pressure gradient, and the Lorentz force, which is the starting point of our coordinates derivation. The MHD equilibrium condition enables to use SPEC equilibria as support for the Boozer coordinates transformation.

In a previous report, we had introduced the magnetic shear in stellarators, and and studied its dependence on magnetic axis torsion and flux surfaces ellipticity [Gui22]. In addition, certain shearless configurations have shown great confinement properties [LP22]. It is hence of interest to determine wether or not the two properties of quasi-symmetry and being shearless are related. Thus, it is important to define a measure to quantify correctly the property of quasi-symmetry. Then this metric has to be evaluated over a region of the space of configurations where the shearless property happens to be present. This way, one would be able to exhibit a correlation if there is one.

Most results about specific magnetic coordinates, as straight field line (SFL) and Boozer coordinates, how they are derived from general poloidal and toroidal angles, are reviewed in II. The starting point, that is the derivation of SFL coordinates, is reviewed in II A. The developement leading to Boozer coordinates starting from SFL ones is done in II B. Then, mathematical derivation of the magnetic field strength $\|B\|$ in several coordinate systems is done with the objective to emphasize the hidden symmetries mentioned previously in II C. Afterwards, a brief development demonstrates how we can constrain the study of our parameters to a narrower space - see II D. Finally quasi-symmetry is introduced formally and a metric to quantify it is presented in II E. Regarding correlation between shearless property and weak quasi-symmetry metric value, it is treated in III.

* salomon.guinchard@epfl.ch
† Swiss Plasma Center, Ecole Polytechnique Fédérale de Lausanne, Lausanne, Suisse

II. THEORY

A. General magnetic coordinates and transformation to straight field lines coordinates

Let us take the ideal situation where the surfaces of constant pressure are nested. The innermost surface is a line and corresponds to the magnetic axis. Let also θ, $\phi \in [0, 2\pi]$ be arbitrary poloidal and toroidal angles. Take (p, θ, ϕ) as coordinate-system, where p is the pressure. The choice of p as an independent radial coordinate can be justified by the assumption made of a non chaotic equilibrium in the volume enclosed by each magnetic surface, and that all magnetic surfaces (that is surfaces of constant pressure p) are nested. We seek coordinate systems in which magnetic field lines are straight, so that the math is simpler, and since they constitute the starting point to the Boozer coordinates transformation, which is fundamental to understand hidden symmetries of stellarators. Those symmetries are said to be hidden since they are symmetries of the magnetic field modulus, and are coordinate-system dependent. Let us now derive several expressions for the magnetic field $\mathbf{B}$ in various coordinate systems.

From the ideal-MHD equation

$$\mathbf{j} \times \mathbf{B} = \nabla p, \tag{1}$$

one can deduce that

$$\begin{aligned} \mathbf{B} \cdot \nabla p = 0, \\ \mathbf{j} \cdot \nabla p = 0. \end{aligned} \tag{2}$$

Making use of Eq.(2), one can expand $\mathbf{B}$ in a basis orthogonal to ∇p, that is for example $\Big\{(\nabla p \times \nabla \theta), (\nabla \phi \times \nabla p)\Big\}$. This yields to

$$\mathbf{B} = B_1(p, \theta, \phi)(\nabla p \times \nabla \theta) + B_2(p, \theta, \phi)(\nabla \phi \times \nabla p). \tag{3}$$

Now using the Maxwell's equation $\nabla \cdot \mathbf{B} = 0$ implies

$$\begin{aligned} & \nabla \cdot \Big(B_1(\nabla p \times \nabla \theta) + B_2(\nabla \phi \times \nabla p)\Big) = 0 \\ \iff & \nabla B_1 \cdot (\nabla p \times \nabla \theta) + \nabla B_2 \cdot (\nabla \phi \times \nabla p) = 0. \end{aligned} \tag{4}$$

Making use of the fact that

$$\nabla B_\alpha(p, \theta\phi) = \frac{\partial B_\alpha}{\partial p} \nabla p + \frac{\partial B_\alpha}{\partial \theta} \nabla \theta + \frac{\partial B_\alpha}{\partial \phi} \nabla \phi, \tag{5}$$

and

$$\nabla p \cdot \Big(\nabla p \times \nabla \theta\Big) = \nabla p \cdot \Big(\nabla \phi \times \nabla p\Big) = 0, \tag{6}$$

$$\nabla \theta \cdot \Big(\nabla p \times \nabla \theta\Big) = \nabla \phi \cdot \Big(\nabla \phi \times \nabla p\Big) = 0, \tag{7}$$

Eq.(4) rewrites

$$\Big(\frac{\partial B_1}{\partial \phi} + \frac{\partial B_2}{\partial \theta}\Big) \nabla p \cdot \Big(\nabla \theta \times \nabla \phi\Big) = 0. \tag{8}$$

We used the cyclic property of the triple product: $\mathbf{a}\cdot(\mathbf{b}\times\mathbf{c}) = \mathbf{c}\cdot(\mathbf{a}\times\mathbf{b}) = \mathbf{b}\cdot(\mathbf{c}\times\mathbf{a})$. One notices that $\nabla p\cdot\Big(\nabla\theta\times\nabla\phi\Big)$ is the jacobian of the coordinate system (p,θ,ϕ), and it can be shown that in such a geometry of nested $\{p = cst\}$ surfaces, it never vanishes, or at least only locally if so. Hence, Eq.(8) implies:

$$\Big(\frac{\partial B_1}{\partial\phi} + \frac{\partial B_2}{\partial\theta}\Big) = 0, \qquad\qquad \forall\phi,\theta\in[0,2\pi]. \tag{9}$$

Since B_1 and B_2 are 2π periodic in θ and ϕ, we can write:

$$\begin{aligned}
&\int_0^{2\pi}\frac{\partial B_1}{\partial\phi}d\theta = \frac{\partial}{\partial\phi}\int_0^{2\pi} B_1 d\theta = 0 \quad \forall\phi\\
&\implies \int_0^{2\pi} B_1 d\theta = g(p)\\
&\implies \int_0^{2\pi}\Big(B_1 - \frac{g(p)}{2\pi}\Big)d\theta = 0\\
&\implies B_1 = \frac{\partial f}{\partial\theta} + \frac{g(p)}{2\pi}.
\end{aligned} \tag{10}$$

The same way, one gets that

$$\begin{aligned}
&\int_0^{2\pi}\frac{\partial B_2}{\partial\theta}d\phi = \frac{\partial}{\partial\theta}\int_0^{2\pi} B_2 d\phi = 0 \quad \forall\theta\\
&\implies \int_0^{2\pi} B_2 d\phi = h(p)\\
&\implies \int_0^{2\pi}\Big(B_2 - \frac{h(p)}{2\pi}\Big)d\phi = 0\\
&\implies B_2 = -\frac{\partial f}{\partial\phi} + \frac{h(p)}{2\pi},
\end{aligned} \tag{11}$$

for some $f(p,\theta,\phi)$, $h(p)$, $g(p)$, where the minus sign before $\partial f/\partial\phi$ in Eq.(11) arises for convenience. Let us define now

$$\psi'(p) = \frac{g(p)}{2\pi}, \quad \chi'(p) = \frac{h(p)}{2\pi}, \quad \text{and} \quad \lambda(p,\theta,\phi) = \frac{f(p,\theta,\phi)}{\psi'(p)}. \tag{12}$$

Then,

$$\begin{aligned}
B_1(p,\theta,\phi) =& \psi'(p)\Big(1 + \frac{\partial\lambda}{\partial\theta}(p,\theta,\phi)\Big)\\
B_2(p,\theta,\phi) =& \chi'(p) - \psi'(p)\frac{\partial\lambda}{\partial\phi}(p,\theta,\phi),
\end{aligned} \tag{13}$$

where the prime denotes the derivative with respect to the pressure p. Recall that

$$\begin{aligned}
\mathbf{B} &= B_1(\nabla p\times\nabla\theta) + B_2(\nabla\phi\times\nabla p)\\
&= \psi'\Big(1 + \frac{\partial\lambda}{\partial\theta}\Big)(\nabla p\times\nabla\theta) + \Big(\chi' - \psi'\frac{\partial\lambda}{\partial\phi}\Big)(\nabla\phi\times\nabla p).
\end{aligned} \tag{14}$$

Since $\psi\equiv\psi(p)$ and $\chi\equiv\chi(p)$, it is possible to write the following:

$$\begin{aligned}\nabla\chi &= \frac{\partial\chi}{\partial p}\nabla p = \frac{d\chi}{dp}\nabla p = \chi'\nabla p\\ \nabla\psi &= \frac{\partial\psi}{\partial p}\nabla p = \frac{d\psi}{dp}\nabla p = \psi'\nabla p.\end{aligned} \tag{15}$$

Plugging Eq.(15) in Eq.(14), one obtains for $\mathbf{B}$:

$$\begin{aligned}\mathbf{B} &= \psi'\Big(1+\frac{\partial\lambda}{\partial\theta}\Big)(\nabla p\times\nabla\theta) + \Big(\chi' - \psi'\frac{\partial\lambda}{\partial\phi}\Big)(\nabla\phi\times\nabla p)\\ &= \Big(\nabla\psi\times\nabla\theta\Big) - \frac{\partial\lambda}{\partial\theta}\Big(\nabla\theta\times\nabla p\Big)\psi' - \Big(\nabla\chi\times\nabla\phi\Big) + \frac{\partial\lambda}{\partial\phi}\Big(\nabla\psi\times\nabla\phi\Big)\\ &= \Big(\nabla\psi\times\nabla\theta\Big) - \frac{\partial\lambda}{\partial\theta}\Big(\nabla\theta\times\nabla\psi\Big) + \nabla\phi\times\nabla\chi\\ &- \frac{\partial\lambda}{\partial\phi}\Big(\nabla\phi\times\nabla\psi\Big) - \frac{\partial\lambda}{\partial p}\Big(\nabla p\times\nabla\psi\Big)\\ &= \Big(\nabla\psi\times\nabla\theta\Big) + \Big(\nabla\psi\times\nabla\lambda\Big) + \Big(\nabla\phi\times\nabla\chi\Big)\\ &= \nabla\psi\times\nabla\Big(\theta+\lambda\Big) + \nabla\phi\times\nabla\chi.\end{aligned} \tag{16}$$

For the last step we used that $\nabla\psi \propto \nabla p$ to add zero with the term $\partial\lambda/\partial p(\nabla p\times\nabla\psi)$. Finally, setting $\theta+\lambda=\theta_s$, $\mathbf{B}$ reads:

$$\mathbf{B} = \nabla\psi\times\nabla\theta_s + \nabla\phi\times\nabla\chi. \tag{17}$$

Note that Eq.(17) gives a contravariant expression for the field $\mathbf{B}$.

One can interpret ψ and χ as toroidal and poloidal magnetic fluxes respectively. Indeed:

$$\begin{aligned}\int_{\phi=cst}\mathbf{B}\cdot\mathbf{n}dS &= 2\pi\psi \equiv 2\pi\psi(p)\\ \int_{\theta=cst}\mathbf{B}\cdot\mathbf{n}dS &= 2\pi\chi \equiv 2\pi\chi(p).\end{aligned} \tag{18}$$

So Eq.(28) enables to conclude that poloidal and toroidal magnetic fluxes are constant on $\{\mathcal{S} : p = cst\}$. Thus, these are called flux surfaces. Hence, we can work with the coordinate system $\{\psi,\theta_s,\phi\}$, and write ψ and χ as follows:

$$\begin{aligned}\psi\equiv\psi(p) &\implies p\equiv p(\psi)\\ \chi\equiv\chi(p) &\implies \chi\equiv\chi(\psi).\end{aligned} \tag{19}$$

With the above representation Eq.(19), one can define the slope of χ along ψ as

$$\frac{d\chi}{d\psi} =: \iota(\psi). \tag{20}$$

Note that ι does also account for the rate of change of the poloidal angle over a toroidal rotation and along a magnetic field line:

$$\begin{aligned}\left.\frac{d\theta}{d\phi}\right|_{\text{along }\mathbf{B}} &= \frac{\mathbf{B}\cdot\nabla\theta}{\mathbf{B}\cdot\nabla\phi} = \frac{\Big(\nabla\psi\times\nabla\theta_s+\nabla\phi\times\nabla\chi\Big)\cdot\nabla\theta_s}{\Big(\nabla\psi\times\nabla\theta_s+\nabla\phi\times\nabla\chi\Big)\cdot\nabla\phi}\\ &= \frac{\Big(\nabla\phi\times\nabla\chi\Big)\cdot\nabla\theta_s}{\Big(\nabla\phi\times\nabla\theta_s\Big)\cdot\nabla\phi}\\ &= \frac{\nabla\chi\cdot\Big(\nabla\theta_s\times\nabla\phi\Big)}{\nabla\psi\cdot\Big(\nabla\theta_s\times\nabla\phi\Big)}\\ &= \frac{d\chi}{d\psi}=\iota\end{aligned} \tag{21}$$

This way, one sees that on flux surfaces, in the plane (ϕ,θ_s), field lines are straight lines:

$$\frac{d\theta_s}{d\phi}=\iota(\psi)\implies\theta_s\propto\phi. \tag{22}$$

Further properties of magnetic coordinates arise from Eq.(1) since

$$\mathbf{j}\times\mathbf{B}=\nabla p\implies\mathbf{j}\cdot\nabla p=0. \tag{23}$$

Recall that

$$\begin{aligned}&\nabla\psi=\psi'\nabla p\quad\&\quad\nabla\chi=\chi'\nabla p\\ \implies&\Big(\nabla\psi\times\nabla\theta_s\Big)\cdot\nabla p=\Big(\nabla\phi\times\nabla\psi\Big)\cdot\nabla p=0.\end{aligned} \tag{24}$$

So $\mathbf{j}$ can be expanded in the basis $\{\Big(\nabla\psi\times\nabla\theta_s\Big),\Big(\nabla\phi\times\nabla\psi\Big)\}$. This enables to write

$$\mu_0\mathbf{j}=J_1\Big(\nabla\psi\times\nabla\theta_s\Big)+J_2\Big(\nabla\phi\times\nabla\psi\Big). \tag{25}$$

Using the fact that $\nabla\cdot\mathbf{j}=0$, and following the same procedure as in Eq.(10,11), one obtains

$$\begin{aligned}J_1(\psi,\theta_s,\phi)=&I'(\psi)-\frac{\partial K}{\partial\theta_s}(\psi,\theta_s,\phi),\\ J_2(\psi,\theta_s,\phi)=&-G(\psi)+\frac{\partial K}{\partial\phi}(\psi,\theta_s,\phi).\end{aligned} \tag{26}$$

Here $K(\psi,\theta_s,\phi)$, $I'(\psi)$, $G'(\psi)$ are analogous to f, g and h respectively. This way,

$$\begin{aligned}&\mu_0\mathbf{j}=\nabla\times\Big(I\nabla\theta_s+G\nabla\phi+K\nabla\psi\Big)=:\nabla\times\mathbf{B},\\ &\mathbf{B}=I\nabla\theta_s+G\nabla\phi+K\nabla\psi+\nabla H.\end{aligned} \tag{27}$$

where H plays the role of a spatial integration constant. The previous equation gives a covariant expression for the magnetic field. Regarding the interpretation of I and G, they carry information about poloidal and toroidal current, since using Ampère's law and previous expressions,

$$\begin{aligned}\oint_{\{\psi,\phi\}=cst} \mathbf{B}\cdot d\mathbf{r} &= 2\pi I(\psi),\\ \oint_{\{\psi,\theta\}=cst} \mathbf{B}\cdot d\mathbf{r} &= 2\pi G(\psi).\end{aligned} \tag{28}$$

Thus, the integral along a contour of constant ϕ corresponds to μ_0 times the toroidal current inside the flux surface determined by ψ, whereas the integral along a contour of constant θ is equal to μ_0 times the poloidal current between this surface and infinity [Hel14].

B. Boozer coordinates derivation - following [Hel14]

Boozer coordinates are the basis for advanced stellarator designs - quasi-axisymmetric (QA), quasi -helical-symmetric (QH), quasi isodynamic (QI). This set of coordinates is particularly useful for the study of the motion of particles in integrable magnetic fields with closed and nested flux-surfaces. Indeed, in these coordinates, motion around the guiding center only depends on the variation of magnetic field and electrostatic potential. The guiding center Lagrangian in Boozer coordinates, as introduced in [CS97] reads

$$\mathcal{L}_{gc} = \Big(mu\frac{B_\psi}{B}\Big)\dot{\psi} + \Big(e\frac{\psi}{c} + mu\frac{B_{\theta_b}}{B}\Big)\dot{\theta_b} + \Big(e\frac{A_{\phi_b}}{c} + mu\frac{B_{\phi_b}}{B}\Big)\dot{\phi_b} - h, \tag{29}$$

where $B = \|B\|$, $\mathbf{A}$ the vector potential evaluated at the guiding center position, h the Hamiltonian, m the mass and u the parallel velocity. Moreover, in Boozer coordinates, the angular dependance of all quantities that appear in Eq.(29) depends on the angular dependance of $\|B\|$. Let us now introduce the outline for the coordinates transformation leading to Boozer coordinates.

i) Start from general poloidal and toroidal angles θ and ϕ.

ii) Change θ to get straight field lines in the plane (ϕ,θ): $\theta \to \theta_s = \theta + \lambda$.

iii) Note that ϕ was left intact: for each ϕ, $\exists\ \theta_s$ leading to $\mathbf{B}$ s.t

$$\mathbf{B} = \nabla\psi \times \nabla\theta_s + \nabla\phi \times \nabla\chi. \tag{30}$$

iv) Change from (θ_s, ϕ) to (θ_b, ϕ_b) by mean of the difference between the initial and final toroidal angles $\nu := \phi_b - \phi$ such that $\theta_b = \theta_s + \iota\nu$. This way, the covariant expression for $\mathbf{B}$ Eq.(27) should be preserved (minus the integration constant):

$$\mathbf{B} = I\nabla\theta_b + G\nabla\phi_b + K\nabla\psi. \tag{31}$$

Moreover, the lines orthogonal to $\mathbf{B}$ and tangent to flux surfaces (that is lines colinear to $\mathbf{B}\times\nabla\psi$), are straight in Boozer coordinates.

We shall now proceed to the derivation. We follow the process by Helander [Hel14]. Recall Eq.(27):

$$\mathbf{B} = I\nabla\theta_s + G\nabla\phi + K\nabla\psi + \nabla H. \tag{32}$$

Now write

$$\begin{aligned} \theta_s &= \theta' + \iota\omega, \\ \phi &= \phi' + \omega, \end{aligned} \tag{33}$$

where $\omega \equiv \omega(\psi, \theta_s, \phi)$ is well behaved and periodic in θ_s, ϕ. Recall also that Eq.(17):

$$\mathbf{B} = \nabla\psi \times \nabla\theta_s + \nabla\phi \times \nabla\chi. \tag{34}$$

Starting from Eq.(34),

$$\begin{aligned} \nabla\theta_s &= \nabla\left(\theta' + \iota\omega\right) = \nabla\theta' + \iota\nabla\omega + \omega\nabla\iota, \\ \nabla\phi &= \nabla\left(\phi' + \omega\right) = \nabla\phi' + \nabla\omega, \end{aligned} \tag{35}$$

we use that

$$\nabla\omega = \frac{\partial\omega}{\partial\psi}\nabla\psi + \frac{\partial\omega}{\partial\theta_s}\nabla\theta_s + \frac{\partial\omega}{\partial\phi}\nabla\phi \qquad \text{and} \qquad \nabla\iota = \frac{\partial\iota}{\partial\psi}\nabla\psi. \tag{36}$$

Moreover, note that

$$\iota = \frac{d\chi}{d\psi} \implies \nabla\chi = \iota\nabla\psi. \tag{37}$$

Plugging these expressions into Eq.(34), one gets

$$\mathbf{B} = \nabla\psi \times \Big(\nabla\theta' + \iota\nabla\omega + \omega\nabla\iota\Big) + \Big(\nabla\phi' + \nabla\omega\Big) \times \nabla\chi. \tag{38}$$

Now, replacing $\nabla\omega$ by its expression from Eq.(36), and identifying the arising terms with ι as in Eq.(37), one gets the following:

$$\begin{aligned} \mathbf{B} =& \nabla\psi \times \Big(\nabla\theta' + \iota\frac{\partial\omega}{\partial\psi}\nabla\psi + \iota\frac{\partial\omega}{\partial\theta_s}\nabla\theta_s + \iota\frac{\partial\omega}{\partial\phi}\nabla\phi\Big) \\ &+ \Big(\nabla\phi' + \frac{\partial\omega}{\partial\psi}\nabla\psi + \frac{\partial\omega}{\partial\theta_s}\nabla\theta_s + \frac{\partial\omega}{\partial\phi}\nabla\phi\Big) \times \Big(\nabla\chi \propto \nabla p \propto \nabla\psi\Big). \end{aligned} \tag{39}$$

Using that $\nabla\chi = \iota\nabla\psi$ and $\nabla a \times \nabla b = -\nabla b \times \nabla a$,

$$\begin{aligned} \mathbf{B} =& \nabla\psi \times \Big(\nabla\theta' + \iota\frac{\partial\omega}{\partial\theta_s}\nabla\theta_s + \iota\frac{\partial\omega}{\partial\phi}\nabla\phi\Big) \\ &+ \nabla\phi' \times \nabla\chi + \Big(\frac{\partial\omega}{\partial\theta_s}\nabla\theta_s + \frac{\partial\omega}{\partial\phi}\nabla\phi\Big) \times \Big(\nabla\chi \propto \nabla\psi\Big) \\ =& \nabla\psi \times \nabla\theta' + \nabla\phi' \times \nabla\chi. \end{aligned} \tag{40}$$

Note that $\mathbf{B}$ in Eq.(40) takes the contravariant form as in Eq.(34). Now, take Eq.(32) and insert $\nabla\theta_s(\theta')$:

$$\begin{aligned} \mathbf{B} &= I\nabla\theta + G\nabla\phi + K\nabla\psi + \nabla H \\ &= I\Big(\nabla\theta' + \iota\nabla\omega + \omega\nabla\iota\Big) + G\Big(\nabla\phi' + \nabla\omega\Big) + K\nabla\psi + \nabla H \\ &= I\nabla\theta' + G\nabla\phi' + \Big(K + I\omega\frac{\partial\iota}{\partial\psi}\Big)\nabla\psi + \iota I\nabla\omega + G\nabla\omega + \nabla H. \end{aligned} \tag{41}$$

In Eq.(41), we used that $\omega\nabla\iota = \omega\partial\iota/\partial\psi\nabla\psi$ to go from second to third line. Now, using the trick of rewriting 0 as $0 = a - a$ in the previous expression for $\mathbf{B}$, we obtain:

$$\begin{aligned}\mathbf{B} =& I\nabla\theta' + G\nabla\psi' + K\nabla\psi + \left[\omega\Big(i\frac{\partial\iota}{\partial\psi} + \iota\frac{\partial I}{\partial\psi} - \iota\frac{\partial I}{\partial\psi}\Big)\nabla\psi\right] \\ &+ \left[\nabla H + \iota I\nabla\omega + \nabla\left(\iota I\right) - \nabla\left(\iota I\right) + G\nabla\omega - \omega\nabla G + \omega\nabla G\right].\end{aligned} \tag{42}$$

Rearranging the terms between brackets yields to

$$\mathbf{B} = I\nabla\theta' + G\nabla\phi' + \left[K - \omega\frac{\partial}{\partial\psi}\Big(\iota I + G\Big)\right]\nabla\psi + \nabla H + \nabla\left[\Big(\iota I + G\Big)\omega\right]. \tag{43}$$

Thus, it is finally possible to write

$$\mathbf{B} = I\nabla\theta' + G\nabla\phi' + K'\nabla\psi + \nabla H', \tag{44}$$

with

$$\begin{aligned}K' &= K - \omega\frac{\partial}{\partial\psi}\Big(\iota I + G\Big) \\ H' &= H + \Big(\iota I + G\Big)\omega.\end{aligned} \tag{45}$$

Now, the boozer coordinates ($\theta' = \theta_b, \phi' = \phi_b$) are chosen such that $H' = 0$. Note that

$$\begin{aligned}H' \equiv 0 \implies \nabla H' = 0 &\implies H + \Big(\iota I + G\Big)\omega = 0 \\ &\iff \omega = -\frac{H}{\iota I + G}.\end{aligned} \tag{46}$$

Hence, the Boozer coordinates transformation can be written as

$$\begin{aligned}\theta_s \longrightarrow \theta_b &= \theta_s + \iota\frac{H}{\iota I + G}, \\ \phi \longrightarrow \phi_b &= \phi + \frac{H}{\iota I + G}.\end{aligned} \tag{47}$$

Recall from Eq.(28) that $I \propto I_{tor}$ and $G \propto I_{pol}$. Thus, it allows us the following interpretation:

$$\mathbf{B} \sim I_{tor}\nabla\theta' + I_{pol}\nabla\phi' + K'\nabla\psi + \nabla(\text{Integration cst } H') \tag{48}$$

H' can indeed be seen as an integration constant, that has to vanish in Boozer coordinates.

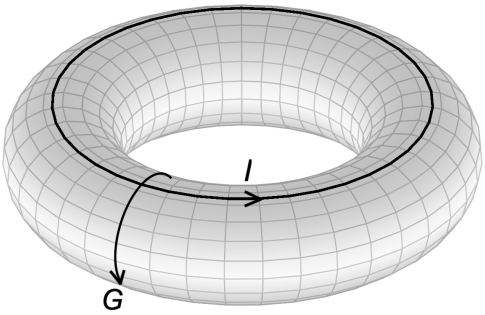

FIG. 1. Poloidal and toroidal currents I and G from the developments above for the outermost surface of a toroidal device

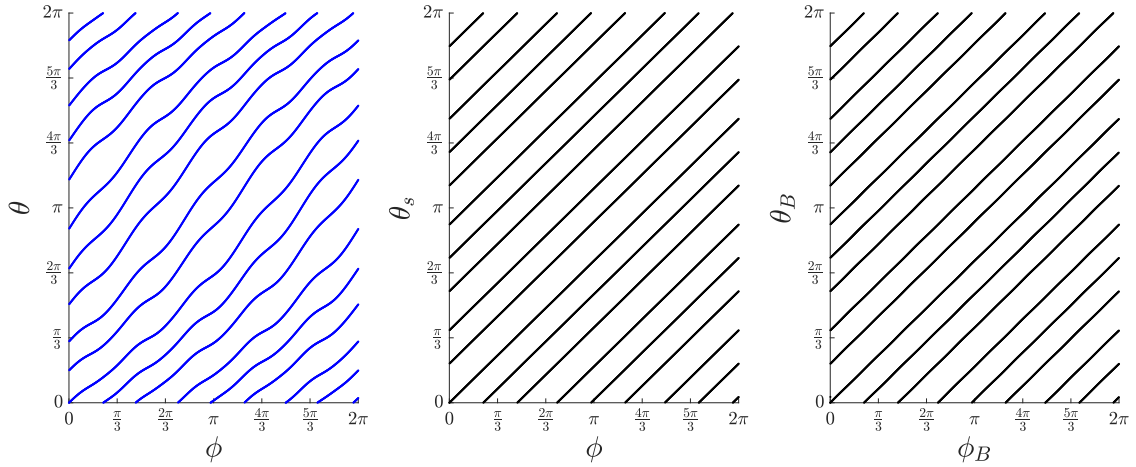

FIG. 2. One magnetic field line plotted over 11 toroidal periods for a random configuration in (e, τ) plane ($R_{11} = 0.24, R_{10} = 0.04$), in different sets of coordinates, starting from the origin

To sum up with the two coordinate systems introduced previously (SFL and Boozer), Fig.(2) shows a magnetic field line plotted over 11 toroidal periods, for one random configuration in the torsion-ellipticity plane. One can note that the behavior of the line is as expected: in the SFL (θ_s, ϕ) magnetic coordinates, the field line is indeed straight, that is θ_s is linear in ϕ. Identical behavior is observed in Boozer coordinates (θ_b, ϕ_b), which coincides with the theory. Note that the represented field line is the same in the three coordinate systems.

C. Fourier coefficients for $\|B\|$ in several coordinate systems

Since for the numerically implemented Boozer coordinates transformation, we needed as an input the Fourier modes of $\|B\|$ [SHW$^+$00], we proceed below to their mathematical derivation. Let us write $\|B\|$ in the form of its Fourier series, as a function of any poloidal and toroidal angles θ and ϕ:

$$\|B\| = \sum_{m,n} B_{mn} \cos(m\theta - n\phi). \tag{49}$$

Recall that for a real function f, one has that its Fourier series converges to the function itself, reading:

$$
\begin{aligned}
f(x) &= \sum_n \hat{f}_n e^{2\pi i n \frac{x}{T}}, \\
\hat{f}_n &:= \frac{1}{T}\int_0^T f(x) e^{-2\pi i n \frac{x}{T}}.
\end{aligned}
\tag{50}
$$

Thus, one obtains the following for the Fourier coefficients of $\|B\|$:

$$
B_{mn} = \frac{1}{2\pi}\frac{N_{fp}}{2\pi}\int_0^{2\pi/N_{fp}}\int_0^{2\pi} d\theta d\phi \|B\|(\theta,\phi) e^{-2\pi i\left(m\frac{\theta}{2\pi}+n\frac{N_{fp}\phi}{2\pi}\right)}. \tag{51}
$$

Hence, dropping the (θ,ϕ) dependence for the sake of simplicity, omitting the integration boundaries, and using a trigonometric relation:

$$
\begin{aligned}
\iint \|B\|\cos(m'\theta - n' N_{fp}\phi) &= \iint \sum_{m,n} B_{mn}\cos(m\theta - nN_{fp}\phi)\cos(m'\theta - n'N_{fp}\phi) d\theta d\phi, \\
&= \sum_{m,n} \iint \|B\|\cos(m\theta - nN_{fp}\phi)\cos(m'\theta - n'N_{fp}\phi) d\theta d\phi.
\end{aligned}
\tag{52}
$$

Using trigonometric identities to transform the cos product, and the fact that

$$
\int_0^1 dt \cos(2\pi n t)\cos(2\pi n' t) = \int_0^1 dt \sin(2\pi n t)\sin(2\pi n' t) = \frac{1}{2}\delta_{nn'}, \tag{53}
$$

$$
\begin{aligned}
&\implies \iint \|B\|\cos(m'\theta - n' N_{fp}\phi) d\theta d\phi \\
&= \sum_{m,n} B_{mn}\Big[\pi\delta_{mm'}\Big\{\int_0^{2\pi/N_{fp}} d\phi \cos(n' N_{fp}\phi)\cos(nN_{fp}\phi) + \int_0^{2\pi/N_{fp}} d\phi \sin(n' N_{fp}\phi)\sin(nN_{fp}\phi)\Big\}\Big] \\
&= \sum_{m,n} B_{mn}\Big[\pi\delta_{mm'}\Big\{\frac{2\pi}{N_{fp}}\int_0^1 d\phi \cos(2\pi n'\phi)\cos(2\pi n\phi) + \frac{2\pi}{N_{fp}}\int_0^1 d\phi \sin(2\pi n'\phi)\sin(2\pi n\phi)\Big\}\Big] \\
&= \frac{2\pi^2}{N_{fp}}\delta_{mm'}\delta_{nn'}B_{mn} \\
&= \frac{2\pi^2}{N_{fp}}B_{m'n'}.
\end{aligned}
\tag{54}
$$

Hence, one obtains a direct expression for the Fourier coefficients:

$$
B_{mn} = \frac{N_{fp}}{2\pi^2}\iint \|B\|\cos(m\theta - nN_{fp}\phi) d\theta d\phi. \tag{55}
$$

The Fourier modes of $\|B\|$ can also be expressed in terms of straight field lines (SFL) (θ_s,ϕ_s), and as a verification of our numerical implementation, in Boozer (θ_b,ϕ_b) coordinates. Recall, that for a bijective and C^1 vector field $\mathbf{v}: U \to V$ s.t $\mathbf{v}(s,t) = (x,y)$, for any $f: V \to \mathbb{R}$ integrable

$$\iint_U f(\mathbf{v}(s,t))|\det(J_{\mathbf{v}}(s,t))|dsdt = \iint_V f(x,y)dxdy. \tag{56}$$

Denoting by $\mathbf{g}_s(\theta,\phi) = (\theta_s,\phi_s)$ the coordinates transformation from geometric to (SFL), one gets that

$$\begin{aligned} B^s_{mn} &= \frac{N_{fp}}{2\pi^2}\iint \|B\|(\theta_s,\phi_s)\cos(m\theta_s - n\phi_s)d\theta_s d\phi_s, \\ &= \frac{N_{fp}}{2\pi^2}\iint \|B\|(\theta,\phi)\cos(m\theta - n\phi)|\det J^s_{\mathbf{g}}(\theta,\phi)|d\theta d\phi, \end{aligned} \tag{57}$$

where $J^s_{\mathbf{g}}(\theta,\phi)$ denotes the jacobian matrix of the coordinates transformation $\mathbf{g}_s$. We recall now the definition $\mathbf{g}_s$:

$$\begin{aligned} &\theta \to \theta_s = \theta + \lambda(\theta,\phi), \\ &\phi \to \phi_s \equiv \phi, \end{aligned} \tag{58}$$

with λ defined by its Fourier series:

$$\lambda(\theta,\phi) = \sum_{m=0}^{M_{pol}}\sum_{n=-N_{tor}}^{N_{tor}} \lambda_{mn}\sin(m\theta - n\phi). \tag{59}$$

Thus, writing $\mathbf{g}_s$ as $\mathbf{g}_s(\theta,\phi) = (g_\theta(\theta,\phi), g_\phi(\theta,\phi))$, one gets for $J^s_{\mathbf{g}}$:

$$J^s_{\mathbf{g}}(\theta,\phi) = \begin{pmatrix} \frac{\partial g_\theta}{\partial\theta} & \frac{\partial g_\theta}{\partial\phi} \\ \frac{\partial g_\phi}{\partial\theta} & \frac{\partial g_\phi}{\partial\phi} \end{pmatrix}. \tag{60}$$

Omitting the (θ,ϕ) dependence, $\det J^s_{\mathbf{g}} = \frac{\partial g_\theta}{\partial\theta}\frac{\partial g_\phi}{\partial\phi} - \frac{\partial g_\theta}{\partial\phi}\frac{\partial g_\phi}{\partial\theta}$, and using

$$\begin{aligned} &g_\theta = \theta + \sum_{m=0}^{M_{pol}}\sum_{n=-N_{tor}}^{N_{tor}} \lambda_{mn}\sin(m\theta - n\phi), \\ &g_\phi = \phi, \end{aligned} \tag{61}$$

$$J^s_{\mathbf{g}}(\theta,\phi) = \begin{pmatrix} \frac{\partial g_\theta}{\partial\theta} & \frac{\partial g_\theta}{\partial\phi} \\ 0 & 1 \end{pmatrix}. \tag{62}$$

This way,

$$\left|\det J_{\mathbf{g}}\right| = \left|\frac{\partial g_\theta}{\partial\theta}\right| = \left|1 + \sum_{m=0}^{M_{pol}} m\cdot\sum_{n=-N_{tor}}^{N_{tor}} \lambda_{mn}\cos(m\theta - n\phi)\right|. \tag{63}$$

Hence,

$$B^s_{mn} = \frac{N_{fp}}{2\pi^2}\iint d\theta d\phi\|B(\theta,\phi)\|\left|1 + \sum_{m',n'} m'\lambda_{m'n'}\cos(m'\theta - n'\phi)\right|\cos(m\theta - n\phi). \tag{64}$$

The same process can be applied to deduce an expression for the Fourier modes of $\|B\|$ in Boozer coordinates. This result will indeed be useful to verify the numerical implementation of the coordinates transformation.

$$B^b_{mn} = \frac{N_{fp}}{2\pi^2} \iint \|B\|(\theta,\phi)\cos(m\theta - n\phi)|\det J^b_{\mathbf{g}}(\theta,\phi)|d\theta d\phi. \tag{65}$$

For Boozer coordinates, the transformation from (θ,ϕ) to (θ_b,ϕ_b) is given by Eq.(66).

$$\begin{aligned} g^b_\theta &:= \theta_s + \iota\nu = \theta + \lambda + \iota\nu = \theta - (\theta_s - \theta) + \iota\nu = \theta + \sum_{m,n} (\lambda_{mn} + \iota\nu_{mn})\sin(m\theta - n\phi), \\ g^b_\phi &:= \phi + \nu = \phi + \sum_{m,n} \nu_{mn}\sin(m\theta - n\phi), \end{aligned} \tag{66}$$

where we used that in the case of a stellarator symmetric configuration, $\nu = \sum_{m,n}\nu_{mn}\sin(m\theta - n\phi)$. The determinant of the jacobian of $\mathbf{g}_b$ can then be computed explicitly to give B^b_{mn}.

$$J^b_{\mathbf{g}}(\theta,\phi) = \begin{pmatrix} \frac{\partial g^b_\theta}{\partial\theta} & \frac{\partial g^b_\theta}{\partial\phi} \\ \frac{\partial g^b_\phi}{\partial\theta} & \frac{\partial g^b_\phi}{\partial\phi} \end{pmatrix}, \tag{67}$$

which gives in terms of matrix coefficients

$$\begin{aligned} J^b_{\mathbf{g}_{11}} &= 1 + \sum_{m,n} m\,(\lambda_{mn} + \iota\nu_{mn})\cos(m\theta - n\phi), \\ J^b_{\mathbf{g}_{12}} &= -\sum_{m,n} n\,(\lambda_{mn} + \iota\nu_{mn})\cos(m\theta - n\phi), \\ J^b_{\mathbf{g}_{21}} &= \sum_{m,n} m\nu_{mn}\cos(m\theta - n\phi), \\ J^b_{\mathbf{g}_{22}} &= 1 - \sum_{m,n} n\nu_{mn}\cos(m\theta - n\phi). \end{aligned} \tag{68}$$

The jacobian determinant then reads

$$\begin{aligned} \left|\det J^b_{\mathbf{g}}\right| =& \left|J^b_{\mathbf{g}_{11}}J^b_{\mathbf{g}_{22}} - J^b_{\mathbf{g}_{12}}J^b_{\mathbf{g}_{21}}\right| \\ =& \Big| - \Big[1 + (\lambda_{mn} + \iota\nu_{mn})\Big]\Big[n'\,(\lambda_{m'n'} + \iota\nu_{m'n'})\Big]\Big[m''\nu_{m''n''}\Big]\Big[1 - n'''\nu_{m'''n'''}\Big] \\ & \cdot\cos(m\theta - n\phi)\cos(m'\theta - n'\phi)\cos(m''\theta - n''\phi)\cos(m'''\theta - n'''\phi)\Big| \end{aligned} \tag{69}$$

where we used Einstein's summation convention in Eq.(69). The above result can then be inserted in Eq.(65) to obtain the coefficients.

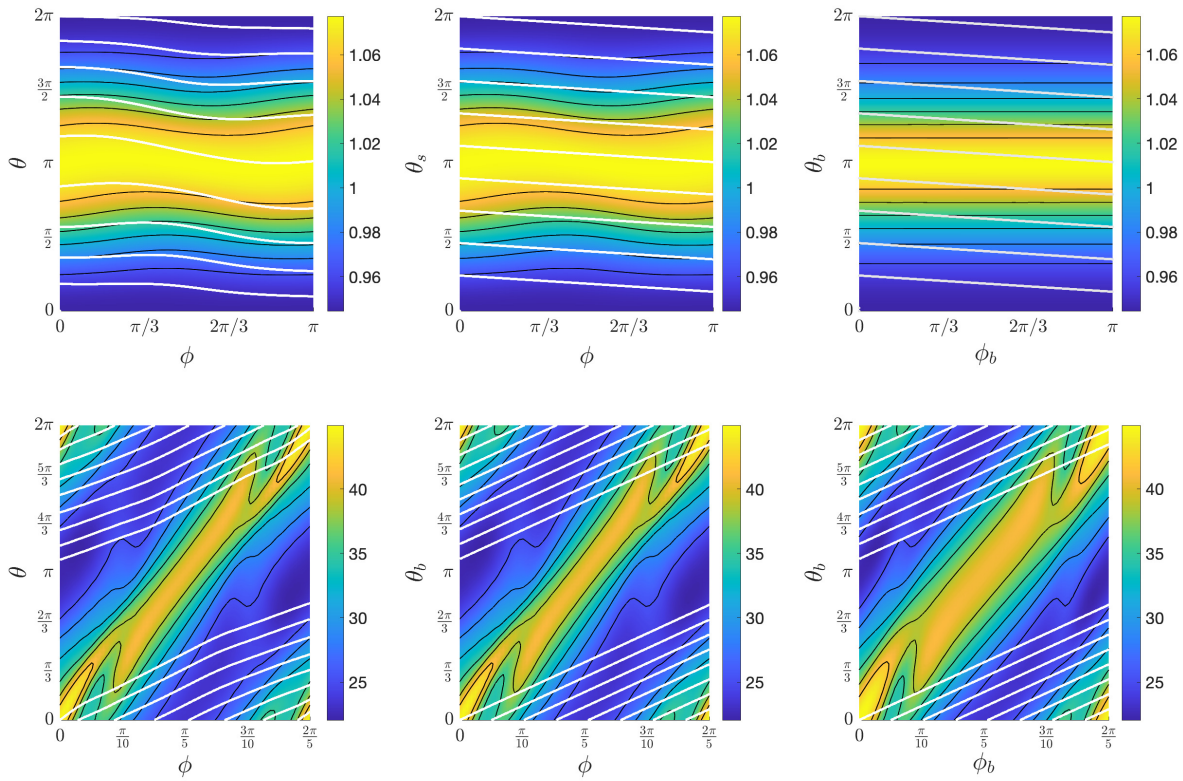

FIG. 3. $\|B\|$ and a field line plotted in general (θ, ϕ), SFL (θ_s, ϕ_s) and Boozer (θ_b, ϕ_b) coordinates for the QA configuration from Fig.(6) (Up) and the QH configuration from Fig.(5) (Down)

D. Central symmetry

Below we show that we can constrain any ellipticity-torsion based study to the half plane $[0, e_{\max}] \times [-\tau_{\max}, \tau_{\max}]$. As our numerical studies in the ellipticity-torsion plane are conducted using SPEC, the previous half plane is written as $[0, R_{11}^{\max}] \times [-R_{10}^{\max}, R_{10}^{\max}]$. We had $R_{11}^{\max} = 0.3$ and $R_{10}^{\max} = 2$. Indeed, there is a central symmetry around the origin. Assume furthermore *stellarator-symmetry* (pure cosine series for the plasma boundary). Take a general (θ, ϕ) coordinate system and assume that any Fourier mode is zero apart from R_{10} and R_{11}:

$$\begin{aligned} R(\theta,\phi) &= R_0 + R_{10}\cos(N_{fp}\phi) + R_{11}\cos(\theta - N_{fp}\phi), \\ Z(\theta,\phi) &= Z_{10}\cos(N_{fp}\phi) + Z_{11}\cos(\theta - N_{fp}\phi). \end{aligned} \tag{70}$$

Setting now $R_{10}, Z_{10} \longrightarrow -R_{10}, -Z_{10}$ and $R_{11}, Z_{11} \longrightarrow -R_{11}, -Z_{11}$, one obtains for the parametrisation:

$$\begin{aligned} \tilde{R}(\theta,\phi) &= R_0 - R_{10}\cos(N_{fp}\phi) - R_{11}\cos(\theta - N_{fp}\phi), \\ \tilde{Z}(\theta,\phi) &= -Z_{10}\cos(N_{fp}\phi) - Z_{11}\cos(\theta - N_{fp}\phi). \end{aligned} \tag{71}$$

which rewrites (using sine and cosine symmetries)

$$\begin{aligned} \tilde{R}(\theta,\phi) &= R_0 + R_{10}\cos(N_{fp}\phi + \pi) + R_{11}\cos(\theta - N_{fp}\phi + \pi) = R(\theta, \phi + \pi), \\ \tilde{Z}(\theta,\phi) &= +Z_{10}\cos(N_{fp}\phi + \pi) + Z_{11}\cos(\theta - N_{fp}\phi + \pi) = Z(\theta, \phi + \pi). \end{aligned} \tag{72}$$

which is equivalent to have rotated the system of π around the origin. Fig.(4) confirms the above development as the magnetic shear has been scanned over the full plane $[-R_{11}^{\max}, R_{11}^{\max}] \times [-R_{10}^{\max}, R_{10}^{\max}]$, showing the central symmetry discussed previously.

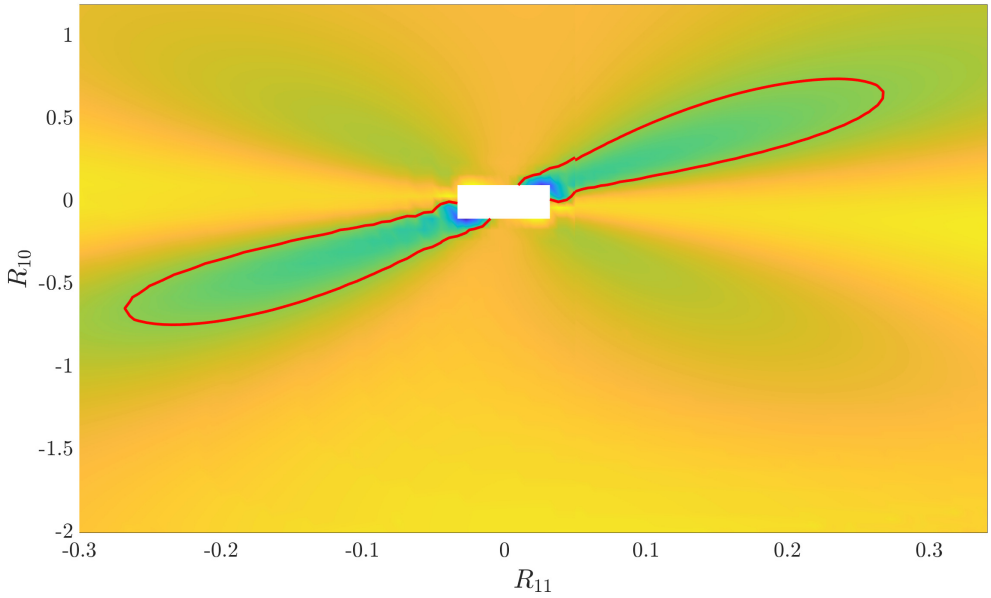

FIG. 4. Magnetic shear scanned over the full plane emphasising the central symmetry discussed above. The white region around the origin corresponds to a zone of non-convergence of the SPEC code.

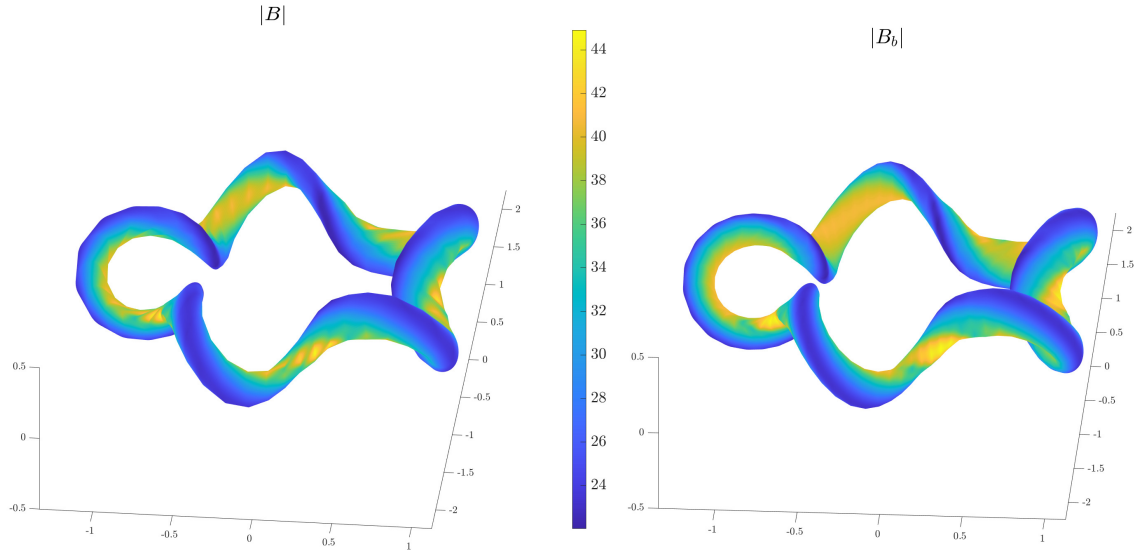

FIG. 5. A quasi-helical symmetric configuration (QH) in general (θ, ϕ) (Left) and Boozer (θ_b, ϕ_b) (Right) coordinates. The color plot shows the amplitude of the magnetic field $\|B\|$.

E. A measure of quasi-symmetry

Quasisymmetric stellarators are an attractive class of optimized magnetic confinement devices to achieve nuclear fusion [RPB21, RSB21]. Practically, the property of quasi-symmetry - that we shall denote by QS from now on - is approximate. It is thus necessary to define a metric in the space of configurations to quantify the departure from the exact QS. The definition of such a metric is not unique, and its expression may be dependent of the choice of magnetic coordinates. One of the commonly used metric to quantify QS is the so-called triple product formulation of QS:

$$f_T = \nabla\psi \times \nabla B \cdot \nabla\big(\mathbf{B} \cdot \nabla B\big), \tag{73}$$

where ψ denotes the usual radial coordinate defined by flux surfaces, and f the letter to refer to the metric. In Boozer coordinates, the triple product metric f_T takes the following form:

$$f_T^b = \big[\partial_{\theta_b} B \partial_{\phi_b} - \partial_{\phi_b} B \partial_{\theta_b}\big]\big(\partial_{\phi_b} + \iota\partial_{\theta_b}\big)B. \tag{74}$$

It follows that $\partial_{\phi_b} B / \partial_{\theta_b} B$ must be a flux function, and hence that B has an explicit symmetry. The property of QS as defined by Boozer [Boo] and Rodríguez *et al.* [RSB21] then naturally arises. It may be expressed as follows: a magnetic field is QS if and only if its magnitude can be written as a function $B(\psi, M\theta_b - N\phi_b)$, with $M, N \in \mathrm{Z}$. Generally, we define the helicity as $\alpha = N/M$ and the helical angle $\xi = \theta_b - \alpha\phi_b$. With these definitions, it is customary to define the so-called *minimal measure* [RPB21]:

$$f_B = \sum_{\substack{m,n \\ n \neq \alpha m}} |B_{mn}|^2. \tag{75}$$

Here B_{mn} denotes the Fourier coefficients of B in Boozer coordinates as in Eq.(65) However, Eq.(75) can be adapted to the desired type of QS. Indeed, the metric that characterises the distance to exact quasi-axisymmetry (QA) will not be the same as to characterise exact quasi helical-symmetry (QH). We define them as follow:

$$\begin{aligned} f_{QA} &= \sum_{n \neq 0} \frac{|B_{mn}|^2}{|B_{00}|^2}, \\ f_{QH} &= \sum_{n \neq \alpha m} \frac{|B_{mn}|^2}{|B_{00}|^2}. \end{aligned} \tag{76}$$

In this report, they will be both reviewed in the plane ellipticity-torsion by mean of the SPEC code, that is, both metric will be scanned over the plane (R_{11}, R_{10}), for SPEC equilibria with one volume devoid of current. In a previous report, we had scanned the magnetic shear $s = \partial\iota/\partial r$, which had enabled to show shearless-regions [Gui22]. Scanning different metrics on the same plane has as main motivation to determine wether there is a correlation between *shearless* and QS, that is $\{s = 0\}$ and $\{f_\alpha \sim 0, \alpha = \text{QA, QH}\}$. Nevertheless, the previous condition has to be taken carefully, since only two Fourier modes have been taken into account to parametrise the plasma boundary in the SPEC code [LHN16]. So the above correlation can be written as follows

$$\{s = 0\}_{R_{11}, R_{10}} \overset{?}{\longleftrightarrow} \{f_\alpha \simeq 0, \alpha = \text{QA, QH}\}_{R_{11}, R_{10}}. \tag{77}$$

Fig.(5)-(6) show respectively a QH and a QA configurations, optimized for the metrics defined as in Eq.(76). The magnitude of $\mathbf{B}$ has been plotted over the plasma boundary in both general and Boozer coordinates, so that the symmetry of $\|B\|$ over each field period is visible. The QA configuration has $N_{fp}^{\text{QA}} = 2$ whereas the QH has $N_{fp}^{\text{QH}} = 5$.

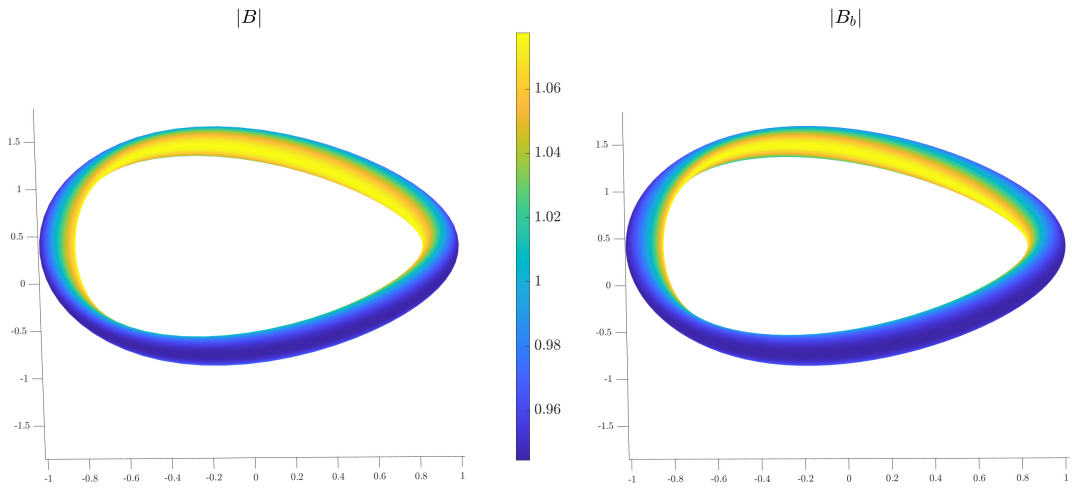

FIG. 6. A quasi-axisymmetric configuration (QA) in general (θ, ϕ) (Left) and Boozer (θ_b, ϕ_b) (Right) coordinates

III. RESULTS

A. On the correlation between the shear and the metrics f_{QH} and f_{QA}

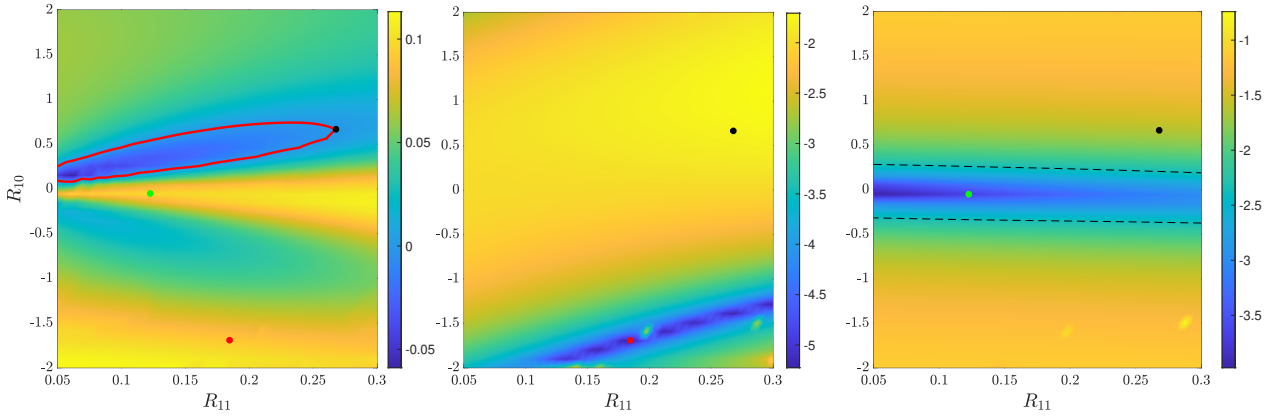

FIG. 7. Left: Magnetic shear s in the plane (R_{11}, R_{10}) (red curve $\equiv \{s = 0\}$). Middle: $\log_{10}(f_{QH})$ in the same plane. Right: $\log_{10}(f_{QA})$ in the same plane.

Fig.(7) shows the magnetic shear s in the plane ellipticity-torsion (R_{11}, R_{10}), as well as the quasi-helical symmetry and quasi-axisymmetry metrics f_{QH} and f_{QA} respectively. Three configurations have been chosen to be studied, in order to confirm or infirm the correlation condition Eq.(77). Recall that the main objective was to determine wether or not we could have QS properties whenever we had the shearless $s = 0$ condition fulfilled. Recall also that the closer the metric is to zero, the closer the configuration is to be QS. This way, one immediately sees that the zones of weak metric (on the middle and right figures) do not match the red curve from the left plot. Hence, we are in measure to rule out the bijection for the correlation type in Eq.(77). However, it is not sufficient to state that the two sets are not correlated. Indeed, one might have to consider more Fourier modes to describe the plasma boundary and the magnetic axis, and hence the study should be made on a less constrained space.

However, in order to verify that our choice of metric remains consistent, even though we could not see any correlation, the magnetic field strength has been evaluated in Boozer coordinates for the three configurations mentioned above. One shearless configuration has been taken (black dot), and compared to one configuration with $f_{\mathrm{QH}} \sim 0$ (red dot) and one with $f_{\mathrm{QA}} \sim 0$ (green dot).

The results are shown in Fig.(8). The left plot shows $\|B\|$ for the shearless configuration, in Boozer coordinates. Comparing it with the configuration marked with a red dot, that is the one with $f_{\mathrm{QH}} \sim 0$, and the central plot of Fig.(8), one sees that it is not exactly QH. Nevertheless, it is visually closer from QH than the shearless configuration (recall that Fig.(3) provides an example of a QH config.). The same comparison can be made for the parametrisation such that $f_{\mathrm{QA}} \sim 0$ (marked with a green dot). Although it is not exactly QA, it is also visually closer to the QA property than the shearless one.

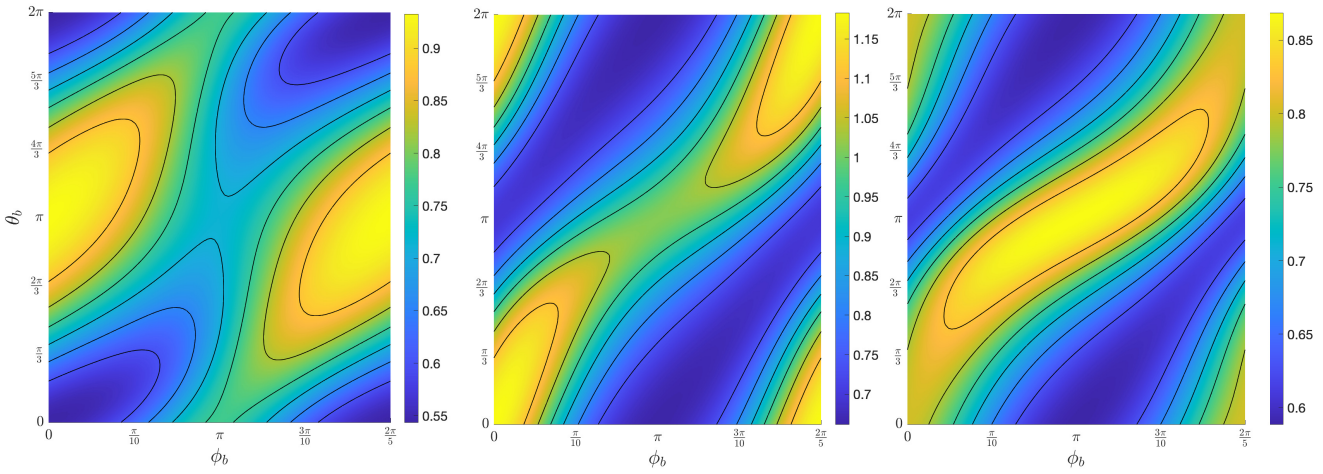

FIG. 8. $\|B\|$ in Boozer coordinates for several configurations from the plane (R_{11}, R_{10}). Left: corresponds to the black dot on Fig.(7) - Middle: red dot - Right: green dot

One further comment can be made about the QA property. According to [LS18, LSP19, PLH19], for any magnetic axis torsion τ, there is a magnetic surface ellipticity e associated such that the resulting configuration is QA, or at least close to be. The right plot of Fig.(7) (f_{QA}) confirms the previous statement. The two dashed lines represent a contour of constant f, emphasising that $\{f_{\mathrm{QA}} \sim 0\}$ wanders the hole plane - recall the central symmetry of any quantity parametrised by (R_{11}, R_{10}) around $(0, 0)$ (see II D).

IV. CONCLUSION

In this report, different sets of magnetic coordinates have been introduced. Straight field lines coordinates as well as the so-called Boozer coordinates have been formally derived starting from common poloidal and toroidal angles. The numerical implementation of these two sets of coordinates enabled to illustrate the concept of quasi symmetry through several particular examples, as a quasi-axisymmetric and a quasi-helical symmetric configurations.

Implementation of a metric to quantify the deviation from quasi-symmetry over the plane of ellipticity and torsion permitted to rule out any bijection between the two properties of quasi-symmetry and constant rotational transform profile, that is shearless configuration. Indeed, when we introduced Eq.(77) to express a general relation between those two properties, we wondered wether there would exist a bijection between them, or if the set of quasi-symmetric configuration was included in the set of shearless configurations, as [LP22] had found several shearless configurations showing quasi-symmetry. However, results have demonstrated that there exist shearless configurations such that no quasi-symmetry property can be exhibited.

In order to study if those two properties (shearless and quasi-symmetry) are related in a way, one should explore other dimensions of the space of configurations, since there exists other ways to generate a magnetic axis torsion, than just imposing the Fourier mode R_{10} to be non zero. Other modes defining the plasma boundary influence the torsion, adding dimensions to the space of configurations. We have been able to demonstrate only that there exists no bijection between QS and $\{s = 0\}$. Fig.(9) summarises what situation might have been expected, versus what the observations were.

Others optimisation processes may involve more Fourier modes, as well as the addition of other properties such as *omnigenity* [JPD+22], or the computation of magnetic equilibria with different equilibrium codes (combination SPEC-VMEC for example) to define an *objective function* [LMZ21].

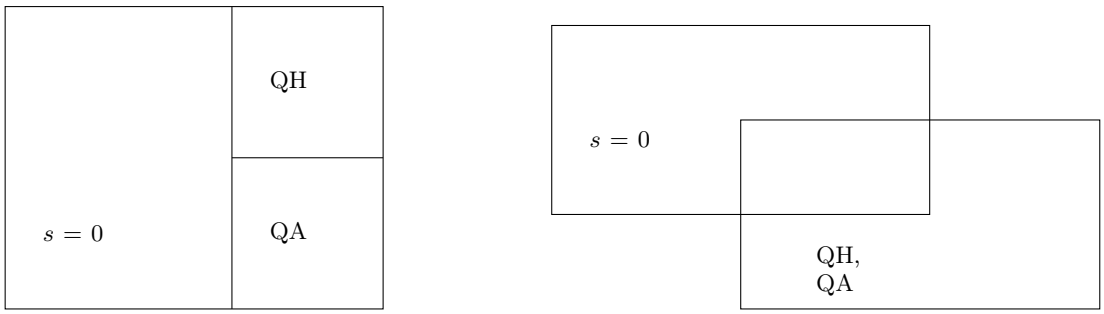

FIG. 9. *Venn diagram* for the correlation between *shearless* property and QS - Left: Hypothesis for the correlation between shearless and QS properties - Right: Conclusion after examination of Fig.(7) and [LP22]

Appendix A: Field line and $\|B\|$ over the full toroidal period of the QH configuration

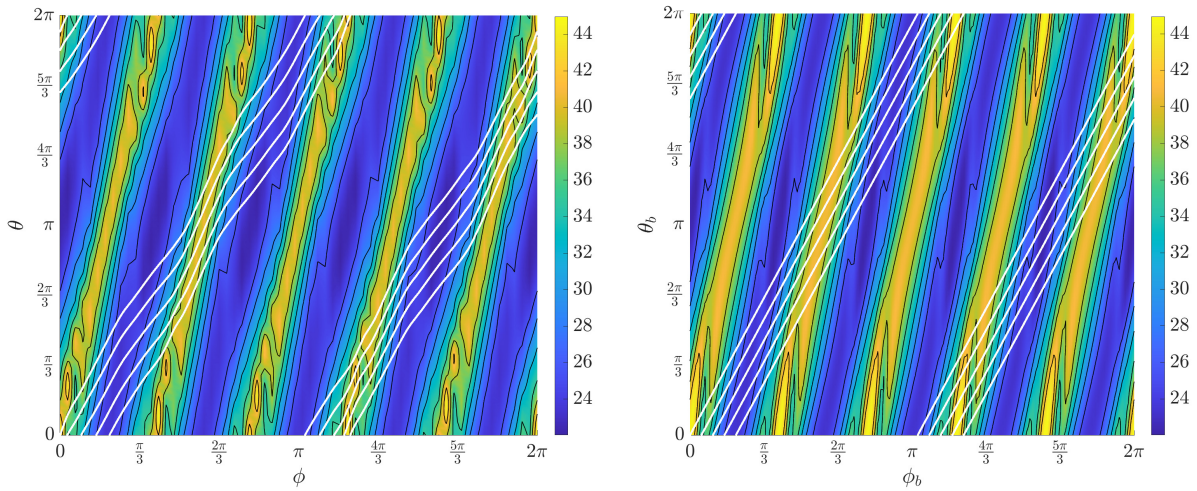

FIG. 10. $\|B\|$ in general (Left) and Boozer (Right) coordinates for the same QH configuration as in Fig.(3). A field-line has been plotted over several periods, and $\|B\|$ is plotted over the full toroidal period in order to emphasise better how the change of coordinate acts on the field-lines. It was difficult to see that the initial field-line was not straight in Fig.(3)

.

[Boo] A H Boozer. Transport and isomorphic equilibria. *Phys. Fluids; (United States)*.

[CS97] John R. Cary and Svetlana G. Shasharina. Omnigenity and quasihelicity in helical plasma confinement systems. *Physics of Plasmas*, 4(9):3323–3333, September 1997.

[Gui22] Salomon Guinchard. Effect of magnetic axis torsion and magnetic surfaces ellipticity on the rotational transform and the magnetic shear, 01 2022.

[Hel14] Per Helander. Theory of plasma confinement in non-axisymmetric magnetic fields. *Reports on Progress in Physics*, 77(8):087001, jul 2014.

[JPD+22] R. Jorge, G. G. Plunk, M. Drevlak, M. Landreman, J. F. Lobsien, K. Camacho Mata, and P. Helander. A single-field-period quasi-isodynamic stellarator, 2022.

[Lan18] Matt Landreman. Booz_xform a numerical implementation of boozer coordinates, 2018.

[LHN16] J. Loizu, S. Hudson, and C. Nührenberg. Verification of the spec code in stellarator geometries. *Physics of Plasmas*, 23:112505, 11 2016.

[LMZ21] Matt Landreman, Bharat Medasani, and Caoxiang Zhu. Stellarator optimization for good magnetic surfaces at the same time as quasisymmetry. *Physics of Plasmas*, 28(9):092505, sep 2021.

[LP22] Matt Landreman and Elizabeth Paul. Magnetic fields with precise quasisymmetry for plasma confinement. *Physical Review Letters*, 128(3), jan 2022.

[LS18] Matt Landreman and Wrick Sengupta. Direct construction of optimized stellarator shapes. part 1. theory in cylindrical coordinates. *Journal of Plasma Physics*, 84(6):905840616, 2018.

[LSP19] Matt Landreman, Wrick Sengupta, and Gabriel G. Plunk. Direct construction of optimized stellarator shapes. part 2. numerical quasisymmetric solutions. *Journal of Plasma Physics*, 85(1):905850103, 2019.

[PLH19] Gabriel G. Plunk, Matt Landreman, and Per Helander. Direct construction of optimized stellarator shapes. part 3. omnigenity near the magnetic axis. *Journal of Plasma Physics*, 85(6):905850602, 2019.

[RPB21] Eduardo Rodriguez, Elizabeth Paul, and Amitava Bhattacharjee. Measures of quasisymmetry for stellarators, 09 2021.

[RSB21] E. Rodríguez, W. Sengupta, and A. Bhattacharjee. Generalized boozer coordinates: A natural coordinate system for quasisymmetry. *Physics of Plasmas*, 28(9):092510, sep 2021.

[RSB22] Eduardo Rodriguez, Wrick Sengupta, and Amitava Bhattacharjee. Topology-mediated approach to the design of quasisymmetric stellarators, 2022.

[SHW+00] R Sanchez, S P Hirshman, A S Ware, L A Berry, and D A Spong. Ballooning stability optimization of low-aspect-ratio stellarators. *Plasma Physics and Controlled Fusion*, 42(6):641–653, may 2000.